Journal of
Composites Science

MDPI

Article

N-Cetyltrimethylammonium Bromide-Modified Zeolite Na-A from Waste Fly Ash for Hexavalent Chromium Removal from Industrial Effluent

Ganesh Kumar Reddy Angaru, Lakshmi Prasanna Lingamdinne, Janardhan Reddy Koduru * and Yoon-Young Chang *

Department of Environmental Engineering, Kwangwoon University, Seoul 01897, Korea
* Correspondence: reddyjchem@gmail.com (J.R.K.); yychang@kw.ac.kr (Y.-Y.C.)

Abstract: Chromium ions released into aquatic environments pose major environmental risks, particularly in developing countries. Here, a low-cost *N*-cetyltrimethylammonium bromide (CTAB)-modified fly ash-based zeolite Na-A (CTAB@FZA) was prepared for the treatment of industrial wastewater contaminated with Cr(VI). CTAB@FZA was evaluated using X-ray diffraction (XRD), Fourier-transform infrared spectroscopy (FT-IR), and scanning electron microscopy (SEM), which showed that CTAB intercalation and coating of the modified zeolite were successful. The effects of influencing variables on the removal of Cr(VI) using CTAB@FZA were also evaluated, including pH, initial concentration, time, temperature, and coexisting ions. Fast adsorption equilibrium was observed after less than 10 min, and CTAB@FZA had a maximum adsorption capacity of 108.76 mg/g and was substantially greater than that of pristine FZA following modification. Furthermore, isothermal and kinetic data demonstrated that Cr(VI) adsorbed onto homogeneous surfaces via rate-limiting monolayer Langmuir adsorption, and according to thermodynamic data, the sorption of the targeted pollutant was exothermic and spontaneous. The application of CTAB@FZA to industrial wastewater treatment yielded Cr(VI) concentrations that were below the USEPA standards. Overall, the findings demonstrated that CTAB@FZA is an effective, promising, and economical adsorbent for the treatment of Cr(VI)-polluted water.

Keywords: *N*-cetyltrimethylammonium bromide; industrial wastewater; kinetic studies; adsorption mechanism

Citation: Angaru, G.K.R.; Lingamdinne, L.P.; Koduru, J.R.; Chang, Y.-Y. *N*-Cetyltrimethylammonium Bromide-Modified Zeolite Na-A from Waste Fly Ash for Hexavalent Chromium Removal from Industrial Effluent. *J. Compos. Sci.* **2022**, *6*, 256. https://doi.org/10.3390/jcs6090256

Academic Editor: Francesco Tornabene

Received: 9 June 2022
Accepted: 1 September 2022
Published: 5 September 2022

1. Introduction

In recent years, various industrial sectors have discharged a substantial volume of metals into the ecosystem in recent years, including plating, metal polishing, papermaking, and leather tanning. The release of Cr ions into aquatic environments poses significant environmental risks, particularly in developing nations [1]. There are two forms of Chromium ions that exist in Cr(VI) and Cr(III), each having its own set of chemical, biological, and environmental characteristics [2]. Cr(VI) is highly soluble, has mobility, and is more poisonous than Cr(III), which is 500-times more toxic and has been linked to cancers, lung diseases, peptic ulcers, vomiting, liver cirrhosis, and neural problems in humans [3]. Furthermore, increased Cr(VI) concentrations have been shown to impede crop and aquatic species growth [3]. Cr(VI) is particularly soluble in aqueous solutions and exists as H_2CrO_4 and dichromate $Cr_2O_7^{2-}$ and is available as $HCrO_4^-$ and CrO_4^{2-} in neutral conditions [4]. Therefore, adsorbents used to remove this harmful metal from the water must have anion-exchange capabilities.

To remove Cr ions from water, scientists have employed adsorption, precipitation, chemical reduction, and ion exchange [5]. Owing to its simplicity, efficacy, lack of sensitivity to harmful compounds, and cost-effectiveness, the adsorption technique is generally preferred [6]. For this, clays, biomass, activated carbon, and zeolites are among the natural

materials that have been employed and evaluated as Cr(VI) adsorbents [4,7–9]. Zeolites, which are crystalline aluminosilicates with structures based on tetrahedral SiO_4 and AlO_4 units joined by shared oxygen atoms, have a strong cation exchange capacity (CEC) [10]. Synthetic zeolites such as ZSM-5, Na-X, Na-A, and Na–Y are often utilized in water remediation [11]. Na-A has a high cation concentration due to its Si/Al ratio being 1, which results in a greater ion exchange capacity. Because of its unique surface area, porosity, high ion exchange capacity, and potent reactivity for hazardous metals, Na-A has been the subject of several of prior studies [12]. Fly ash is a byproduct of coal-fired power stations, and a substantial portion of fly ash is created globally as waste material each year across the world. The leaching of harmful compounds from spilled fly ash into groundwater has made the disposal of this material an urgent environmental concern. For example, fly ash has Al and Si, which are the major elements of natural zeolites coupled with O atoms [13,14]. As a consequence, an economically feasible and widely obtainable aluminosilicate crystal derived from waste fly ash can be used as the raw goods for the synthesis of zeolite; nevertheless, zeolites have some drawbacks. Owing to the negatively charged framework structure of the zeolite, there is very little affinity toward anionic heavy metals [15]. Therefore, modification of zeolite with a cationic surfactant is required. Amine and quaternary ammonium salts are the cationic surfactants. These can provide anion sorption adsorbents with a huge number of positively charged sites. For example, CTAB (*N*-cetyltrimethylammonium bromide), HDTMA (hexadecyltrimethylammonium), APTS (propyl trimethoxy silane), polyethyleneimine [1,16,17], have been successfully used for surface modification [18].

The objective of this research was to mix the cationic surfactant CTAB with the synthesized zeolite Na-A from fly ash (FZA) to increase Cr(VI) removal capability from aqueous solutions. The modification of FZA with CTAB is employed to enhance the reactivity of FZA by changing the surface charge from negative to positive. Cationic exchange and hydrophobic interactions can influence the sorption of a CTAB on the exterior surface of FZA. At a low surfactant loading, the surfactant cations are exchanged with the exchangeable cations of the FZA (i.e., Na^+), forming a monolayer of surfactant cations on the surface. At concentrations above the critical micelle concentration, a bilayer of surfactant molecules (admicelle) is connected to the surface, with the outer layer of surfactant molecules bound by hydrophobic interactions. The surface charge of the FZA is switched from negative to positive oriented in the direction of the solution and now displays Cr(VI) removal efficiency.

Furthermore, using XRD, SEM, and FTIR spectroscopy, the Cr(VI) removal mechanism was explored, and also the removal efficiencies of Cr(VI) from industrial effluents employing CTAB@FZA. Finally, the effects of the pH of the solution, adsorption kinetics, adsorption isotherms, and coexisting ion's effect on Cr(VI) elimination were studied.

2. Experimental Section

2.1. Chemicals

Waste fly ash from Korea South-East Power Co., Ltd.'s Yeongheung thermal power plant located in Heung-myeon, Younggong, Ongjin-gun, Incheon, Republic of Korea was used to synthesize zeolite Na-A. Samchun Pure Chemical Co., Ltd., Seoul, Korea, supplied *N*-cetyltrimethylammonium bromide (99 percent purity), hydrochloric acid, and sodium hydroxide, while Duksan Pure Chemical Co., Ltd., Gyeonggi-do, Korea, supplied K_2CrO_4 for the preparation of Cr(VI) stock solution.

2.2. Synthesis of CTAB@FZA

The Na-A zeolite synthesized from fly ash, as previously described [19], is shown in Figure S1. CTAB@FZA was synthesized using a previously described process with slight modification [20]. Figure 1 shows the modification of zeolite and its application. One hundred mL (0.1 M) CTAB was mixed with 2 g of FZA. After stirring for 24 h, the solution was rinsed with distilled water multiple times and dried overnight at 60 °C.

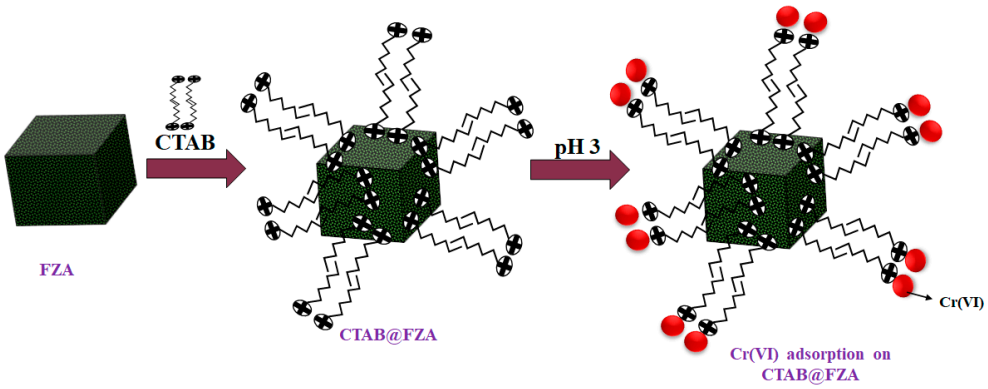

Figure 1. Schematic diagram of CTAB@FZA for Cr(VI) removal.

2.3. Adsorption Experiments

The batch sorption investigations were carried out in a falcon tube (50 mL with 0.5 g/L of CTAB@FZA added to 50 mL of a selected concentration of Cr(VI) at pH 3. The falcon tubes were shaken for the requisite amount of time at 298 ± 3 K using a rotator shaker. A reagent blank (Cr(VI) solution without CTAB@FZA) was used to confirm that the falcon tube had negligible adsorption. Filtration of the adsorbents was accomplished by a 0.45 µm syringe filter. Using an autosampler and inductively coupled plasma-optical emission spectroscopy, the residual levels of both heavy metals in the filtrate were determined (ICP-OES, Avio 200, PerkinElmer, Waltham, MA, USA). The CTAB@FZA's metal uptake capacity (Q_e, mg/g) was determined at equilibrium using the following equation:

$$\text{Adsorption capacity}: \ Q_e = (C_0 - C_e) \times \frac{v}{m}$$

Here C_0 and C_e signify the initial and equilibrium concentrations (mg/L) of adsorbate, respectively, and v and m denote the volume of aqueous solution (L) and weight of adsorbent (g), respectively.

2.4. Sorbent Characterization

The following analytical approach was used to confirm the changes in the surface characteristics of CTAB@FZA. The functional groups on the surface were examined using an FTIR (Cary 610, Agilent, Santa Clara, CA, USA); the changes in surface crystallinity were examined using XRD using a D8 Discover (Bruker AXS, Billerica, MA, USA); and SEM (JEOL, Tokyo, Japan) examination was performed to characterize morphological changes.

3. Results and Discussion

3.1. Characterization

3.1.1. XRD

XRD was employed to determine the crystalline structures of FZA and CTAB@FZA before and after adsorption. Figure 2 depicts the strong, high-intensity peaks in FZA at 2-theta 10–35 °C, which correspond to the components of zeolite Na-A [21]. FZA possesses strong crystallinity, although the diffraction pattern of CTAB@FZA revealed a decrease in the peak intensity. Additionally, the surface became amorphous. It is owing to the modification of FZA with CTAB [22]. Furthermore, the peak at 20.3 °C is attributable to chromium oxide on the CTAB@FZA surface following Cr(VI) adsorption [23,24]. These findings revealed that CTAB successfully modified the zeolite and that Cr(VI) adsorption on CTAB@FZA was successful.

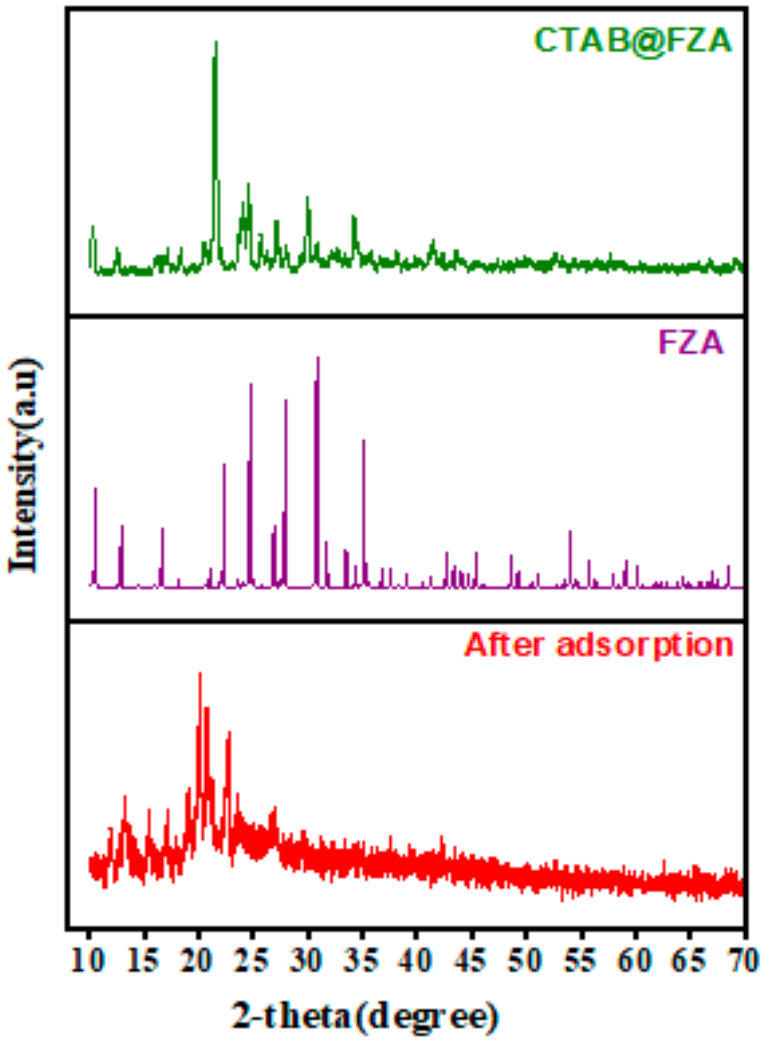

Figure 2. XRD spectra of FZA@CTAB (**top**), FZA (**middle**), and after Cr(VI) adsorption of CTAB@FZA (**bottom**).

3.1.2. FTIR and SEM

FTIR spectroscopic measurements of commercially purchased CTAB, CTAB@FZA, and FZA were undertaken to explore the functional groups on the produced composites, with the findings displayed in Figure 3a. The stretching vibrations of the -CH_3 and -CH_2 groups from CTAB are ascribed to the strong peaks at 2841 and 2916 cm^{-1}, respectively, while the peak at 1470 cm^{-1}, which is attributed to the bending vibrations of NH_4^+, was reduced following loading of the zeolite surface [25].

The peaks at 985, 534, and 454 cm^{-1} are the stretching vibrations of Si-O-Si, Al-O-Si, and Si-O, respectively, on the FZA surface. These peaks shifted to 960, 550, and 449 cm^{-1}, respectively, after surfactant loading. This indicates that these peaks interact with the surfactant on the FZA [26,27]. In addition, the peaks at 970 and 889 cm^{-1} correspond to C-N^+ stretching in the CTAB and slightly shifted on the CTAB@FZA surface [28]. Overall, the results indicate that the CTAB surfactant successfully modified the FZA. Moreover, Figure 3b displays a strong peak at 920 cm^{-1} related to Cr = O after adsorption of Cr(VI) [29], which is evidence of successful sorption.

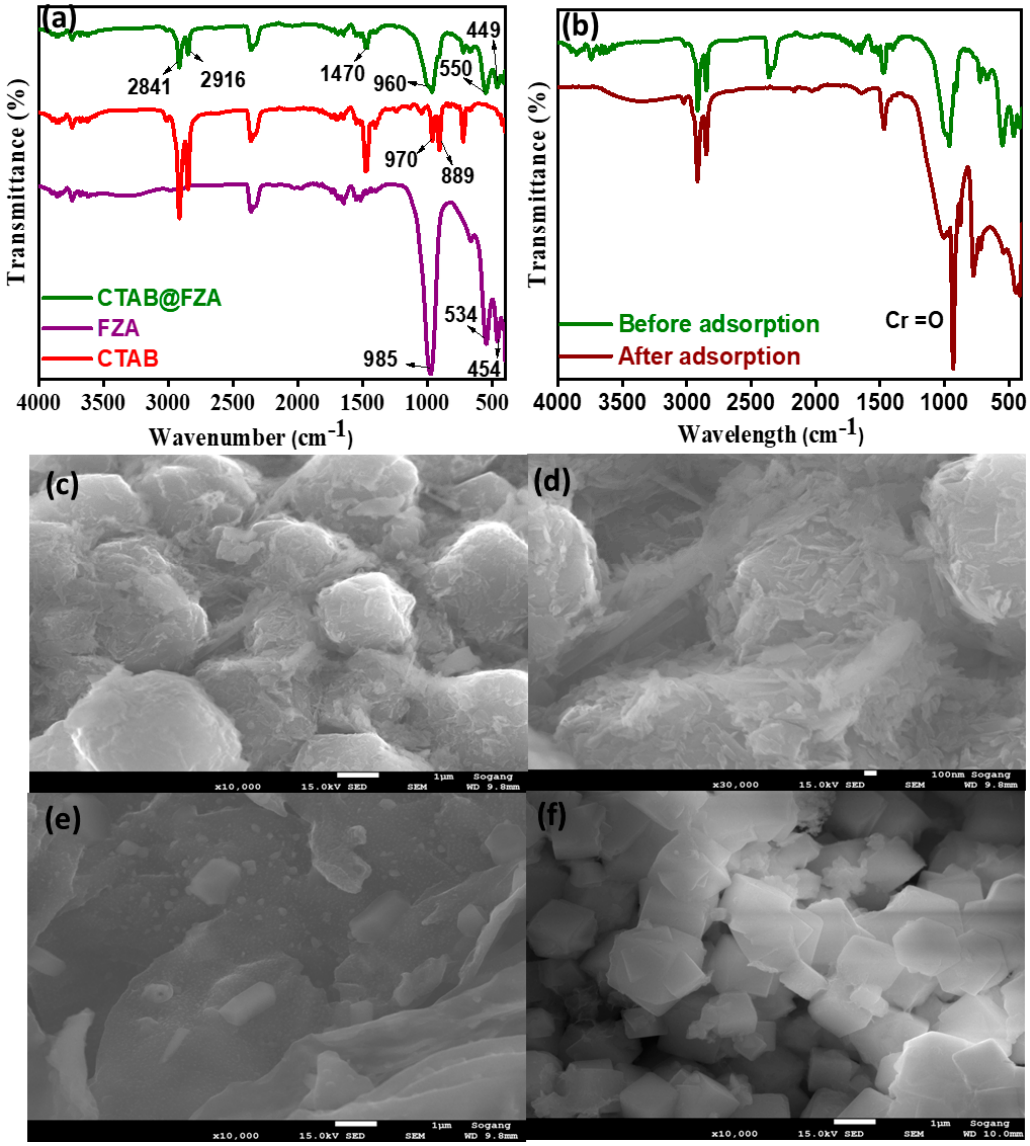

Figure 3. (**a**) FTIR spectra of CTAB@FZA and FZA; (**b**) Before and after Cr(VI) adsorption of CTAB@FZA; (**c**–**e**) scanning electron microscope (SEM) images of CTAB@FZA and (**f**) FZA.

SEM micrographs of the CTAB@FZA and FZA are shown in Figure 3. The rough, irregular surface and pores on the CTAB@FZA (Figure 3c–e) and regular smooth cubic particles of the FZA (Figure 3f) can be seen [30]. For successful modification, the combination of cationic modifier and FZA surface is crucial. Because it leads to high hydrophilicity, surface roughness has a significant impact on sorption efficiency. During the adsorption phase, the CTAB@FZA's uneven surface and pores could have served as Cr(VI) binding sites [31]. These findings further demonstrate the successful modification of the zeolite with CTAB.

3.1.3. BET Surface Area Analysis

The surface area, pore volume, and average pore diameter of CTAB@FZA and FZA are included in Table 1. The CTAB@FZA surface area and total pore volume are 0.78 m^2/g and 0.01 cm^3/g, respectively, which are lower than the pristine FZA (28.46 m^2/g and 0.01 cm^3/g). The decrease in the surface area and pore volume after modification of FZA with CTAB is owing to the CTAB units obstructing several major channels of the FZA, thus impeding the N_2 diffusion via these channels. Furthermore, after CTAB modification, the average pore diameter value rose. The most plausible scenario is that the CTAB blocked

the smallest pore sizes in a higher proportion [32,33]. These findings demonstrated that the CTAB occupied not only the surface but also the pores of the FZA.

Table 1. Surface textural properties of CTAB@FZA and FZA.

Adsorbent	BET Surface Area (m^2/g)	Total Pore Volume (cm^3/g)	Average Pore Diameter (nm)
FZA	28.46	0.04	5.34
CTAB@FZA	0.78	0.01	48.09

3.2. Sorption Batch Experiments Results

3.2.1. Effect of pH

The initial solution pH is crucial in the Cr(VI)-removal process. The adsorbate's initial pH influenced not only the protonation of the functional sites in the CTAB@FZA but also the Cr(VI) speciation. Adsorption efficiency dropped when the initial solution pH increased, as illustrated in Figure 4. In acidic conditions, the major forms of Cr(VI) are $HCrO_4^-$ and $Cr_2O_7^{2-}$ ions. As a result of CTAB@FZA protonation, the adsorbent surface was more positively charged under acidic conditions. Through electrostatic attraction, the adsorbent could effectively adsorb Cr-containing anions, resulting in increased adsorption efficiency [34]. The adsorption capacity decreased at higher pH. This was due to the competition between the anionic adsorbate and OH^- ions and repulsion with a negative surface of adsorbent that occurred during the pH increase [35]. Based on these findings, a pH of 3 was chosen as the optimal pH for further studies.

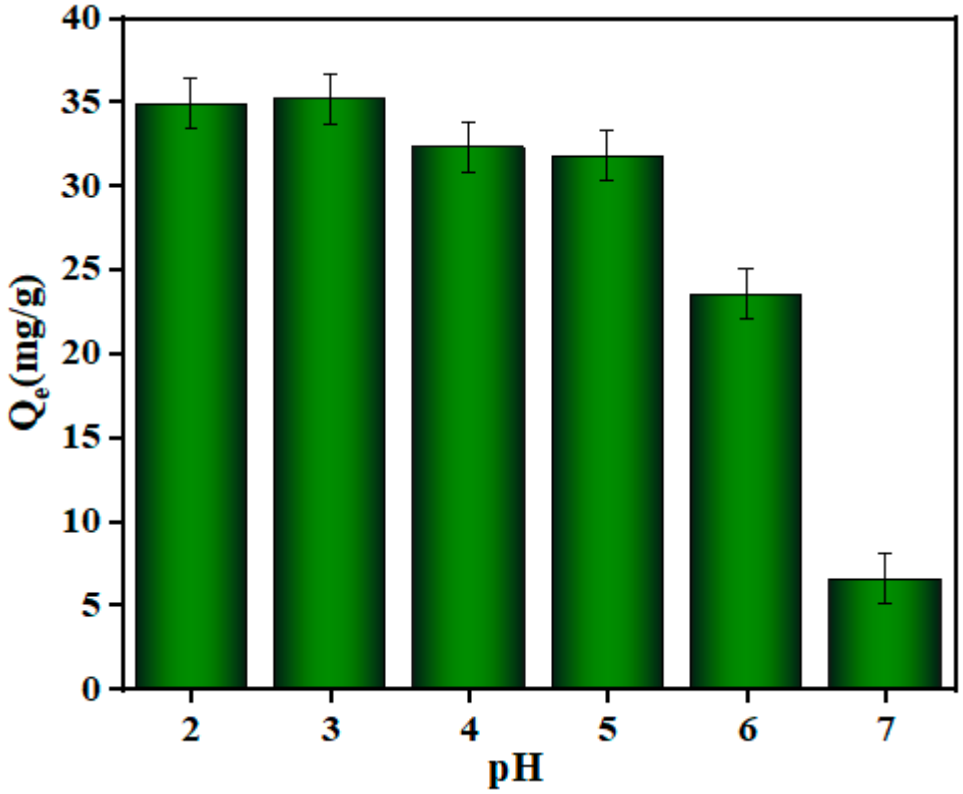

Figure 4. pH effect on Cr(VI) removal from water by CTAB@FZA (initial concentration = 20 mg/L, adsorbent dose = 0.5 g/L, pH = 2–7, time = 10 min, Temperature = 298 K).

3.2.2. Effect of Contact Time and Adsorption

The contact time influence on Cr(VI) removal by the CTAB@FZA was examined. Due to electrostatic interactions between the positively charged CTAB@FZA surface and negatively charged Cr(VI) ions, the CTAB@FZA demonstrated better Cr(VI) adsorption.

The adsorption process was very rapid, with a rising adsorption capacity that reached equilibrium within 10 min. At equilibrium, the sorption efficiency of the CTAB@FZA was 35.22 mg/g. The adsorption kinetics were explored by applying the pseudo-first-order, pseudo-second-order, and Freundlich adsorption kinetics models (Figure 5a and Table 2). The results suggested that the pseudo-second-order model was more favorable than the other models based on a higher correlation coefficient (R^2) of nearly one as well as a better match with the Qe, exp. These findings demonstrate that the rate-determining step could be regulated by the electrostatic interaction between the adsorbent and adsorbate [36].

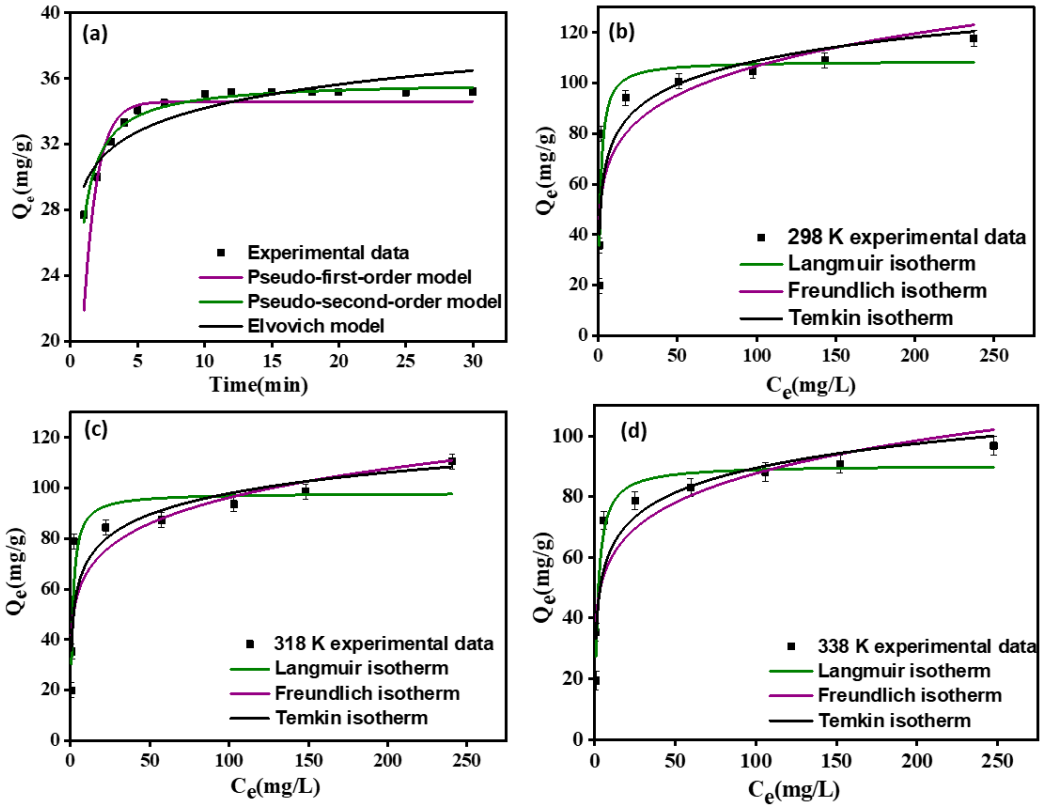

Figure 5. (**a**) Time effect and sorption kinetics (initial concentration = 20 mg/L, time = 1–30 min, and T = 298 K); and the initial concentration effect and sorption isotherms of CTAB@FZA towards Cr(VI) removal at (**b**) 298 K, (**c**) 318 K, and (**d**) 338 K (initial concentration = 10–300 mg/L, contact time = 10 min). Adsorbent dose = 0.5 g/L and pH = 3.

Table 2. Adsorption kinetic parameters of CTAB@FZA towards Cr(VI).

Q_e, exp (mg/g)	Pseudo-First-Order (PFO)			Pseudo-Second-Order (PSO)			Elvovich		
	Qe (mg/g)	K_1 (min^{-1})	R^2	Qe (mg/g)	K_2 (g/mg·min)	R^2	α (mg/g·min)	β (g/mg)	R^2
35.22	34.60	1.00	0.4010	35.64	0.08	0.9723	2.88	0.48	0.8135

3.2.3. Adsorbate Concentration and Adsorption Isotherms

The effect of Cr(VI) concentration on adsorption is shown in Figure 5b–d. The initial concentration was adjusted from 10 to 300 mg/g in the experiments, and the adsorption capacity increased correspondingly associated with a high correlation gradient. However, at high equilibrium concentrations of Cr(VI), the increase in removal efficiency was limited because a passivated layer quickly developed and covered the reactive sites on the adsorbent surface.

The Langmuir, Freundlich, and Temkin adsorption isotherm models were employed to describe the sorption isotherm data (Figure 5b–d), and Table 3 lists the corresponding parameters. The maximum adsorption capacity of CTAB@FZA was 108.76 mg/g at 298 K

whereas unmodified FZA showed a very low adsorption capacity of just 0.42 mg/g (as previously reported) [21]. More over the direct use of CTAB in water treatment is limited because of its solubility in water., However, some researchers used CTAB-modified composites for the successful removal of Cr(VI) from an aqueous solution. For example, Zhang Yu et al. 2019 achieved 76.33 mg/g by surface-modified leaves with CTAB [37], CTAB functionalized double-shelled hollow microspheres were synthesized by Cai et al. 2019 and their maximum adsorption capacity was 202.02 mg/g [38], Cai et al. 2020 were developed MoS_2/CTAB and obtained the adsorption capacity 88.3 mg/g [39], and Li Na et al. 2017 were prepared $MnFe_2O_4$@SiO_2−CTAB, and their adsorption capacity was 25.04 mg/g [1] towards Cr(VI) removal from the water. These findings suggested that the adsorption capacity of CTAB@FZA is comparable and relatively higher than some of CTAB-modified composites and lower compared to CTAB functionalized double-shelled hollow microspheres [38]. However, the modified FZA with CTAB enhances FZA adsorption capacity for Cr(VI) that is expectation of this study. Moreover, CTAB@FZA shows higher adsorption capacity compared to some of FZA-modified materials (Table 4). Additionally, the solid waste flyash-derived zeolite is an economically feasible material as well as could skip the problems of its disposal issues of flyash. However, the modification leads to lower surface area. If improve the surface area of composite may increase adsorption capacity furthermore that may need further or alternative modifications.

Table 3. Sorption isotherm parameters.

Temperature (K)	Langmuir			Freundlich			Temkin		
	Q max (mg/g)	K_L (L/mg)	R^2	K_F (mg/g)(L/mg)$^{1/n}$	n (L/g)	R^2	KT (L/mg)	Bt	R^2
298	108.76	0.81	0.9071	50.15	6.09	0.7789	32.84	13.43	0.842
318	98.1	0.79	0.8805	45.53	6.15	0.7699	34.7	12.00	0.8224
338	90.45	0.54	0.9419	40.51	5.96	0.8141	21.92	11.62	0.8852

Table 4. Comparison of Cr(VI) sorption by different reported adsorbents.

Adsorbent	Q Max (mg/g)	Conditions (pH; Temperature)	Ref
Zeolite/MgAL-LDHs	15.69	6–7; 298 K	[2]
MIL−100(Fe)	30.45	2; 298 K	[40]
Alginate supported Fe/Ni-Zeolite	7.36	3; 298 K	[41]
Ball milled activated carbon	28.90	7; 295 K	[4]
Tectona grandis sawdust biochar	83.50	3; 303 K	[42]
Fe(II)-Natural Zeolite	0.7	4; 298 K	[43]
Surface modified zeolite-Y	1.95	3–4; 298 K	[16]
Rice Husk Ash-Based Zeolite FAU	3.56	5; 298 K	[44]
Amine-Functionalized Zeolite	13.5	3; 298 K	[45]
CTAB@FZA	108.76	3; 298 K	Present study

Moreover 'n' value is greater than 1.0 implies that Cr(VI) shows suitable sorption by CTAB@FZA. In comparison to the Freundlich and Temkin models, the correlation coefficient (R^2) of the Langmuir adsorption isotherm curve (0.9071) demonstrates a superior agreement. These findings revealed that Cr(VI) adsorption on CTAB@FZA was dominated by homogenous surface adsorption, with the adsorption following physisorption of monolayer adsorption patterns [33,36]. Moreover, the CTAB@FZA maximum adsorption capacity was higher than that reported previously (Table 4), indicating the potential use of this adsorbent for the remediation of Cr(VI) contaminated water.

3.2.4. Temperature Effect and Adsorption Thermodynamics

The influence of reaction temperature on the Cr(VI) sorption by CTAB@FZA is depicted in Figure 5b–d. Notably, the adsorption ability decreased with rising reaction temperature. The maximum adsorption capacity was 108.76 mg/g at room temperature (298 k), followed by 98.1, and 90.45 mg/g at 318, and 338 K, respectively. The isotherm data were subsequently used to compute Gibbs free energy (ΔG°), enthalpy (ΔH°), and entropy (ΔS°) from a plotting of ln Kc vs. 1/T (Figure S2), as given in Table 5. The ΔH° is negative revealing that the sorption of Cr(VI) by CTAB@FZA was an exothermic reaction at all three temperatures. Decreasing the degree of randomness of the adsorbed species results in a negative ΔS° value, and the negative ΔG° values reveal that the adsorptive performance of Cr(VI) by CTAB@FZA was spontaneous. However, the change in ΔG° values with increasing temperature demonstrates that substantially lower temperatures were more favorable for the Cr(VI) elimination [46].

Table 5. Adsorption thermodynamic parameters.

Temperature (K)	Q_{max} (mg/g)	ln K_c	ΔG° (KJ/mol)	ΔH° (KJ/mol)	ΔS° (J/K/mol)	R^2
298	108.76	4.48	−11.52			
318	98.1	4.35	−11.11	−12.06	−2.69	0.8825
338	90.45	3.90	−10.96			

3.2.5. Effect of Coexisting Ions

The coexisting anions effect on the elimination of Cr(VI) is depicted in Figure 6. Notably, coexisting cations had no effect on Cr(VI) removal whereas anions did. For example, sulfate and nitrate had an unfavorable effect on the adsorption efficiency of CTAB@FZA at a concentration of 20 mg/L. Because sulfate and nitrate have similar molecular dimensions and hydration degrees as $HCrO_4^-$, this likely reflects competition with $HCrO_4^-$ for adsorption sites, thereby reducing the Cr(VI) removal efficiency [34]. In contrast, the presence of chlorine and phosphate did not affect Cr(VI) removal.

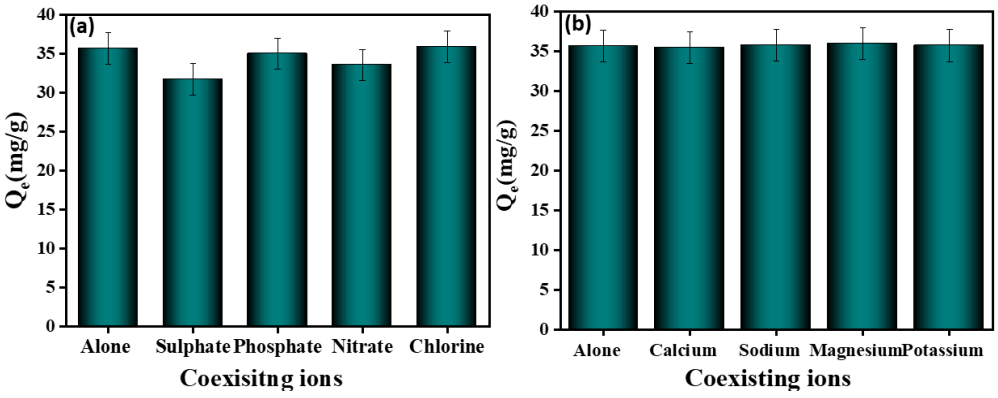

Figure 6. Effects coexisting ions (**a**) anions and (**b**) cations on the Cr(VI) removal from water by CTAB@FZA (Cr(VI) = 20 mg/L, coexisting ions = 20 mg/L, adsorbent dose = 0.5 g/L, pH = 3, time = 10 min, T = 298 K).

3.3. Application of CTAB@FZA for the Elimination of Chromium from Industrial Wastewater

The efficiency of the synthesized CTAB@FZA for chromium removal from industrial water was evaluated using samples from the Banwol and Sihwa industrial sites in the Republic of Korea (Figure 7a,b). Heavy metal ions were abundant in the industrial effluent samples, with a low pH value (pH 1.5). To ensure a homogeneous concentration, the wastewater was vigorously stirred before the adsorption experiments. The suspended debris was then filtered via Whatman filter paper and adjusted the pH of the filtered solution

to 3 to increase the adsorption efficacy. Chromium (3.9 mg/L), calcium (80.2 mg/L), potassium (61.8 mg/L), sodium (39.8 mg/L), fluoride (150 mg/L), chloride (740 mg/L), sulphate (650 mg/L), and phosphate (766 mg/L) were all also present in the industrial effluent.

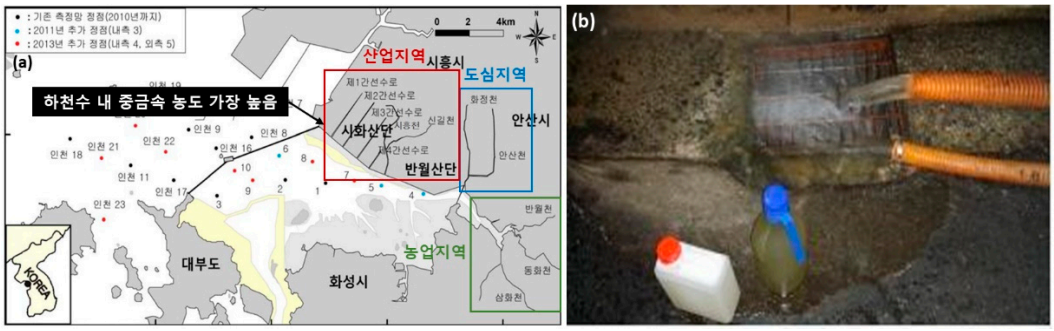

Figure 7. (**a**) Location of Banwol and Sihwa industrial site, and (**b**) Control site for unauthorized discharge of wastewater in industrial complexes.

During the absorption experiments, the concentration of chromium decreased when the contact duration was increased, as shown in Figure 8. It took 240 min to achieve the USEPA surface water permissible standard levels for total chromium (0.1 mg/L) [47,48] and 300 min to attain equilibrium. It could be that because of other competing ions in high concentrations, it took a long time to achieve equilibrium when compared to synthetic water. These overall findings show that CTAB@FZA has the ability to treat industrial wastewater to attain the permitted standard of water quality for chromium.

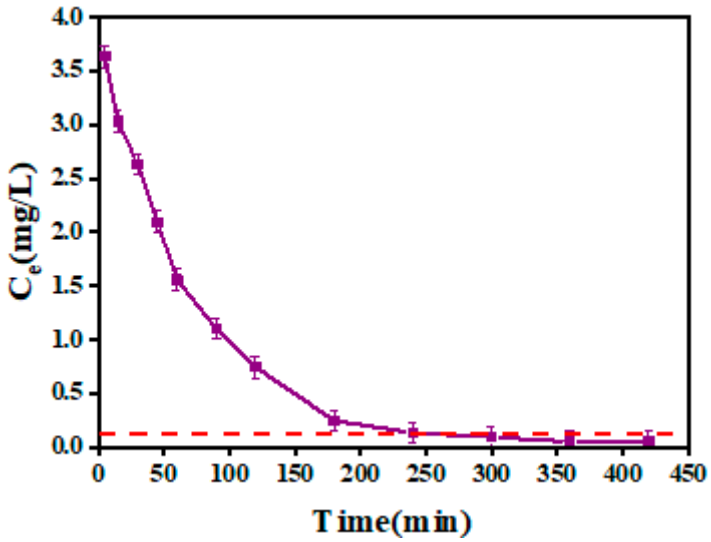

Figure 8. Application of CTAB@FZA for chromium removal from industrial wastewater. The dashed red line indicates the USEPA surface water permissible standard (pH = 3, dose = 0.5 g/L, T = 298 K).

4. Conclusions

The zeolite synthesized from fly ash was modified with CTAB for Cr(VI) removal from water. Zeolite modification was achieved via intercalation and surface coating with CTAB, as confirmed by XRD, FTIR, and SEM examination. The adsorption of Cr(VI) by CTAB@FZA was significantly influenced by solution pH, and acidic conditions were optimal for Cr(VI) uptake. Adsorption was extremely quick and took less than 10 min to achieve equilibrium. The reaction's adsorption kinetics followed a pseudo-second-order model. CTAB@FZA achieved a maximum sorption capacity of 108.76 mg/g, which is relatively high compared to other adsorbents. A thermodynamics analysis revealed that it was reaction was exothermic and spontaneous. Coexisting cations did not influence Cr(VI) uptake, whereas sulfate and nitrate had a negative impact on Cr(VI) removal. Overall,

CTAB@FZA was found to be a superior adsorbent that has significant potential for the efficient and economically viable removal of chromium from industrial wastewater. Even though CTAB@FZA shows higher adsorption capacity compared to some of FZA, was lower than that CTAB functionalized double-shelled hollow microspheres [38] because of decreasing of the surface area of FZA upon modification. However, the limitations of CTAB for water treatment and enhancing FZA adsorbability were achieved by the preparation of CTAB@FZA, which is expected in this study. If improve the surface area or porous of composite by further modification that may increase the adsorption capacity furthermore. Additionally, the solid waste fly ash-derived zeolite is an economically feasible material as well as could skip the problems of its disposal issues of fly ash.

Supplementary Materials: The following supporting information can be downloaded at: https://www.mdpi.com/article/10.3390/jcs6090256/s1, Figure S1: Synthesis of Zeolite from Coal fly ash; Figure S2: (a) Effect of temperature on Cr(VI) removal; (b) Adsorption thermodynamics; Details of isotherms, kinetics, and thermodynamic modeling analysis.

Author Contributions: G.K.R.A. and Y.-Y.C. conceived and designed the experiments; G.K.R.A. contributed to conducting experiments, and data curation; L.P.L. contributed to the interpretation of results and assisted to conduct experiments; G.K.R.A. and J.R.K. conceptualized, analyzed the data, wrote the paper and revised manuscript. Y.-Y.C. contributed analysis tools and edited the proof of the manuscript. All authors have read and agreed to the published version of the manuscript.

Funding: This study was funded by the National Research Foundation, South Korea, through the Ministry of Science and ICT (2021R1F1A106379311) and the Ministry of Education (No. 2021R1A6A1A03038785) to conduct this research. Also funded by the Korea Environmental Industry & Technology Institute (2020002470002).

Institutional Review Board Statement: Not applicable.

Informed Consent Statement: Not applicable.

Data Availability Statement: The data presented in this study are available on request from the corresponding author.

Conflicts of Interest: The authors declare no conflict of interest.

References

1. Li, N.; Fu, J.; Lu, Z.; Ding, Z.; Tang, B.; Pang, J. Facile preparation of magnetic mesoporous $MnFe_2O_4$@SiO_2-CTAB composites for Cr(VI) adsorption and reduction. *Environ. Pollut.* **2017**, *220*, 1376–1385. [CrossRef]
2. Zhang, X.; Gao, J.; Zhao, S.; Lei, Y.; Yuan, Y.; He, C.; Gao, C.; Deng, L. Hexavalent chromium removal from aqueous solution by adsorption on modified zeolites coated with Mg-layered double hydroxides. *Environ. Sci. Pollut. Res. Int.* **2019**, *26*, 32928–32941. [CrossRef]
3. Seliem, M.K.; Mobarak, M. Cr(VI) uptake by a new adsorbent of CTAB–modified carbonized coal: Experimental and advanced statistical physics studies. *J. Mol. Liq.* **2019**, *294*, 111676. [CrossRef]
4. Fang, Y.; Yang, K.; Zhang, Y.; Peng, C.; Robledo-Cabrera, A.; Lopez-Valdivieso, A. Highly surface activated carbon to remove Cr(VI) from aqueous solution with adsorbent recycling. *Environ. Res.* **2021**, *197*, 111151. [CrossRef] [PubMed]
5. Karimi-Maleh, H.; Ayati, A.; Ghanbari, S.; Orooji, Y.; Tanhaei, B.; Karimi, F.; Alizadeh, M.; Rouhi, J.; Fu, L.; Sillanpää, M. Recent advances in removal techniques of Cr(VI) toxic ion from aqueous solution: A comprehensive review. *J. Mol. Liq.* **2021**, *329*, 115062. [CrossRef]
6. Angaru, G.K.R.; Choi, Y.L.; Lingamdinne, L.P.; Koduru, J.R.; Yang, J.K.; Chang, Y.Y.; Karri, R.R. Portable SA/CMC entrapped bimetallic magnetic fly ash zeolite spheres for heavy metals contaminated industrial effluents treatment via batch and column studies. *Sci. Rep.* **2022**, *12*, 3430. [CrossRef] [PubMed]
7. Shakya, A.; Agarwal, T. Removal of Cr(VI) from water using pineapple peel derived biochars: Adsorption potential and re-usability assessment. *J. Mol. Liq.* **2019**, *293*, 111497. [CrossRef]
8. López Zavala, M.Á.; Romero-Santana, H.; Monárrez-Cordero, B.E. Removal of Cr(VI) from water by adsorption using low cost clay-perlite-iron membranes. *J. Water Proc. Eng.* **2020**, *38*, 101672. [CrossRef]
9. Adam, M.R.; Salleh, N.M.; Othman, M.H.D.; Matsuura, T.; Ali, M.H.; Puteh, M.H.; Ismail, A.F.; Rahman, M.A.; Jaafar, J. The adsorptive removal of chromium (VI) in aqueous solution by novel natural zeolite based hollow fibre ceramic membrane. *J. Environ. Manag.* **2018**, *224*, 252–262. [CrossRef]

10. Luo, H.; Law, W.W.; Wu, Y.; Zhu, W.; Yang, E.-H. Hydrothermal synthesis of needle-like nanocrystalline zeolites from metakaolin and their applications for efficient removal of organic pollutants and heavy metals. *Microporous Mesoporous Mater.* **2018**, *272*, 8–15. [CrossRef]
11. Makgabutlane, B.; Nthunya, L.N.; Nxumalo, E.N.; Musyoka, N.M.; Mhlanga, S.D. Microwave Irradiation-Assisted Synthesis of Zeolites from Coal Fly Ash: An Optimization Study for a Sustainable and Efficient Production Process. *ACS Omega* **2020**, *5*, 25000–25008. [CrossRef]
12. Behin, J.; Bukhari, S.S.; Dehnavi, V.; Kazemian, H.; Rohani, S. Using Coal Fly Ash and Wastewater for Microwave Synthesis of LTA Zeolite. *Chem. Eng. Tech.* **2014**, *37*, 1532–1540. [CrossRef]
13. Tauanov, Z.; Shah, D.; Inglezakis, V.; Jamwal, P.K. Hydrothermal synthesis of zeolite production from coal fly ash: A heuristic approach and its optimization for system identification of conversion. *J. Clean. Prod.* **2018**, *182*, 616–623. [CrossRef]
14. Koshy, N.; Singh, D.N. Fly ash zeolites for water treatment applications. *J. Envion. Chem. Eng.* **2016**, *4*, 1460–1472. [CrossRef]
15. Song, W.; Shi, T.; Yang, D.; Ye, J.; Zhou, Y.; Feng, Y. Pretreatment effects on the sorption of Cr(VI) onto surfactant-modified zeolite: Mechanism analysis. *J. Environ. Manag.* **2015**, *162*, 96–101. [CrossRef]
16. Yusof, A.M.; Malek, N.A. Removal of Cr(VI) and As(V) from aqueous solutions by HDTMA-modified zeolite Y. *J. Hazard. Mater.* **2009**, *162*, 1019–1024. [CrossRef]
17. Wang, H.; Zhang, H.; Jiang, J.-Q.; Ma, X. Adsorption of bisphenol A onto cationic-modified zeolite. *Desalin. Water Treat.* **2016**, *57*, 26299–26306. [CrossRef]
18. Jing, X.; Cao, Y.; Zhang, X.; Wang, D.; Wu, X.; Xu, H. Biosorption of Cr(VI) from simulated wastewater using a cationic surfactant modified spent mushroom. *Desalination* **2011**, *269*, 120–127. [CrossRef]
19. Choi, Y.L.; Angaru, G.K.R.; Kim, D.S.; Ahn, H.Y.; Kim, D.H.; Choi, C.D.; Reddy, K.J.; Yang, J.K.; Chang, Y.Y. Preparation of Na-X and Na-A zeolites from coal fly ash in a thermoelectric power plant and comparison of the adsorption characteristics for Cu (II) with a commercial zeolite. *Appl. Chem. Eng.* **2019**, *30*, 749–756.
20. Hosseini Hashemi, M.S.; Eslami, F.; Karimzadeh, R. Organic contaminants removal from industrial wastewater by CTAB treated synthetic zeolite Y. *J. Environ. Manag.* **2019**, *233*, 785–792. [CrossRef]
21. Angaru, G.K.R.; Choi, Y.L.; Lingamdinne, L.P.; Choi, J.S.; Kim, D.S.; Koduru, J.R.; Yang, J.K.; Chang, Y.Y. Facile synthesis of economical feasible fly ash-based zeolite-supported nano zerovalent iron and nickel bimetallic composite for the potential removal of heavy metals from industrial effluents. *Chemosphere* **2021**, *267*, 128889. [CrossRef] [PubMed]
22. Leyva-Ramos, R.; Jacobo-Azuara, A.; Diaz-Flores, P.E.; Guerrero-Coronado, R.M.; Mendoza-Barron, J.; Berber-Mendoza, M.S. Adsorption of chromium(VI) from an aqueous solution on a surfactant-modified zeolite, Colloids and Surfaces A. *Colloids Surf. A Physicochem. Eng. Asp.* **2008**, *330*, 35–41. [CrossRef]
23. Majumder, R.; Sheikh, L.; Naskar, A.; Vineeta; Mukherjee, M.; Tripathy, S. Depletion of Cr(VI) from aqueous solution by heat dried biomass of a newly isolated fungus Arthrinium malaysianum: A mechanistic approach. *Sci. Rep.* **2017**, *7*, 11254. [CrossRef] [PubMed]
24. Dhal, B.; Abhilash; Pandey, B.D. Mechanism elucidation and adsorbent characterization for removal of Cr(VI) by native fungal adsorbent. *Sustain. Envion. Res.* **2018**, *28*, 289–297. [CrossRef]
25. Wang, Y.; Jiang, Q.; Cheng, J.; Pan, Y.; Yang, G.; Liu, Y.; Wang, L.; Leng, Y.; Tuo, X. Synthesis and characterization of CTAB-modified bentonite composites for the removal of Cs^{+}. *J. Radioanal. Nucl. Chem.* **2021**, *329*, 451–461. [CrossRef]
26. Jiang, L.; Ye, Q.; Chen, J.; Chen, Z.; Gu, Y. Preparation of magnetically recoverable bentonite-Fe_3O_4-MnO_2 composite particles for Cd(II) removal from aqueous solutions. *J. Colloid Interface Sci.* **2018**, *513*, 748–759. [CrossRef] [PubMed]
27. Zhou, W.; Wang, H.; Hou, S.; Wang, S. Preparation of Fe_3O_4@SiO_2@MnO_2 microspheres as an adsorbent for Th(IV) removal from aqueous solution. *J. Radioanal. Nucl. Chem.* **2021**, *329*, 253–263. [CrossRef]
28. de Barros, H.R.; Piovan, L.; Sassaki, G.L.; de Araujo Sabry, D.; Mattoso, N.; Nunes, A.M.; Meneghetti, M.R.; Riegel-Vidotti, I.C. Surface interactions of gold nanorods and polysaccharides: From clusters to individual nanoparticles. *Carbohydr. Polym.* **2016**, *152*, 479–486. [CrossRef]
29. Sathvika, T.; Kumar Saraswathi, A.R.; Rajesh, V.; Rajesh, N. Confluence of montmorillonite and Rhizobium towards the adsorption of chromium(vi) from aqueous medium. *RSC Adv.* **2019**, *9*, 28478–28489. [CrossRef]
30. Dovi, E.; Kani, A.N.; Aryee, A.A.; Jie, M.; Li, J.; Li, Z.; Qu, L.; Han, R. Decontamination of bisphenol A and Congo red dye from solution by using CTAB functionalised walnut shell. *Environ. Sci. Pollut. Res. Int.* **2021**, *28*, 28732–28749. [CrossRef]
31. Guan, Q.; Gao, K.; Ning, P.; Miao, R.; He, L. Efficient removal of low-concentration Cr(vi) from aqueous solution by 4A/HACC particles. *New J. Chem.* **2019**, *43*, 17220–17230. [CrossRef]
32. Aloulou, H.; Ghorbel, A.; Aloulou, W.; Ben Amar, R.; Khemakhem, S. Removal of fluoride ions (F(-)) from aqueous solutions using modified Turkish zeolite with quaternary ammonium. *Environ. Technol.* **2021**, *42*, 1353–1365. [CrossRef]
33. Hailu, S.L.; Nair, B.U.; Redi-Abshiro, M.; Diaz, I.; Tessema, M. Preparation and characterization of cationic surfactant modified zeolite adsorbent material for adsorption of organic and inorganic industrial pollutants. *J. Environ. Chem. Eng.* **2017**, *5*, 3319–3329. [CrossRef]
34. Zhang, X.; Li, M.; Su, Y.; Du, C. A novel and green strategy for efficient removing Cr(VI) by modified kaolinite-rich coal gangue. *Appl. Clay Sci.* **2021**, *211*, 106208. [CrossRef]
35. Liang, M.; Ding, Y.; Zhang, Q.; Wang, D.; Li, H.; Lu, L. Removal of aqueous Cr(VI) by magnetic biochar derived from bagasse. *Sci. Rep.* **2020**, *10*, 21473. [CrossRef]

36. Belachew, N.; Hinsene, H. Preparation of cationic surfactant-modified kaolin for enhanced adsorption of hexavalent chromium from aqueous solution. *Appl. Water Sci.* **2019**, *10*, 38. [CrossRef]
37. Zhang, Y.; Li, M.; Li, J.; Yang, Y.; Liu, X. Surface modified leaves with high efficiency for the removal of aqueous Cr(VI). *Appl. Surf. Sci.* **2019**, *484*, 189–196. [CrossRef]
38. Cai, W.; Gu, M.; Jin, W.; Zhou, J. CTAB-functionalized C@SiO_2 double-shelled hollow microspheres with enhanced and selective adsorption performance for Cr(VI). *J. Alloy. Compd.* **2019**, *777*, 1304–1312. [CrossRef]
39. Cai, W.; Dionysiou, D.D.; Fu, F.; Tang, B. CTAB-intercalated molybdenum disulfide nanosheets for enhanced simultaneous removal of Cr(VI) and Ni(II) from aqueous solutions. *J. Hazard. Mater.* **2020**, *396*, 122728. [CrossRef]
40. Forghani, M.; Azizi, A.; Livani, M.J.; Kafshgari, L.A. Adsorption of lead(II) and chromium(VI) from aqueous environment onto metal-organic framework MIL-100(Fe): Synthesis, kinetics, equilibrium and thermodynamics. *J. Solid State Chem.* **2020**, *291*, 121636. [CrossRef]
41. Angaru, G.K.R.; Lingamdinne, L.P.; Choi, Y.L.; Koduru, J.R.; Yang, J.K.; Chang, Y.Y. Encapsulated zerovalent iron/nickel-fly ash zeolite foam for treating industrial wastewater contaminated by heavy metals. *Mater. Today Chem.* **2021**, *22*, 100577. [CrossRef]
42. Vo, A.T.; Nguyen, V.P.; Ouakouak, A.; Nieva, A.; Doma, B.T.; Tran, H.N.; Chao, H.-P. Efficient Removal of Cr(VI) from Water by Biochar and Activated Carbon Prepared through Hydrothermal Carbonization and Pyrolysis: Adsorption-Coupled Reduction Mechanism. *Water* **2019**, *11*, 1164. [CrossRef]
43. Lv, G.; Li, Z.; Jiang, W.T.; Ackley, C.; Fenske, N.; Demarco, N. Removal of Cr(VI) from water using Fe(II)-modified natural zeolite. *Chem. Eng. Res. Des.* **2014**, *92*, 384–390. [CrossRef]
44. Chanda, R.; Hosain, M.; Sumi, S.A.; Sultana, M.; Islam, S.; Biswas, B.K. Removal of Chromium (VI) and Lead (II) from Aqueous Solu-tion Using Domestic Rice Husk Ash-(RHA-) Based Zeolite Faujasite. *Adsorpt. Sci. Technol.* **2022**, *2022*, 4544611. [CrossRef]
45. Nasanjargal, S.; Munkhpurev, B.A.; Kano, N.; Kim, H.J.; Ganchimeg, Y. The removal of chromium (VI) from aqueous solution by amine-functionalized zeolite: Kinetics, thermodynamics, and equilibrium Study. *J. Environ. Prot.* **2021**, *12*, 654–675. [CrossRef]
46. Qiu, Z.; Chen, H.; Wang, Z.; Zhang, T.; Yang, D.; Qiu, F. Efficient removal of As (capital SHA, Cyrillic) via the synergistic effect of oxidation and absorption by FeOOH@MnO_2@CAM nano-hybrid adsorption membrane. *Chemosphere* **2020**, *258*, 127329. [CrossRef]
47. Alley, E.R. *Water Quality Control Handbook*; McGraw-Hill: New York, NY, USA, 2007; Volume 2.
48. Duranoğlu, D.; Buyruklardan Kaya, İ.G.; Beker, U.; Şenkal, B.F. Synthesis and adsorption properties of polymeric and polymer-based hybrid adsorbent for hexavalent chromium removal. *Chem. Eng. J.* **2012**, *181–182*, 103–112. [CrossRef]